Int. J. Electrochem. Sci., 7 **(2012)** 258 - 271

International Journal of
ELECTROCHEMICAL
SCIENCE
www.electrochemsci.org

Effect of Hydrogen Peroxide and Oxalic Acid on Electrochromic Nanostructured Tungsten Oxide Thin Films

H.M.A. Soliman[1,*], *A.B. Kashyout*[1], *Mohamed S. El Nouby*[1], *A.M. Abosehly*[2]

[1]Advanced Technology and New Materials Research Institute, City for Scientific Research and Technology Applications, P.O. Box 21934, New Borg El Arab City, Alexandria, Egypt
[2] Physics Department, Faculty of Science, Al-Azhar University, Al-Azhar Street, P.O. Box. 71524, Assiut, Egypt
[*]E-mail: h.soliman@mucsat.sci.eg

Received: 27 October 2011 / *Accepted:* 5 December 2011 / *Published:* 1 January 2012

Electrochromic tungsten oxide, WO_3, nanomaterials have been prepared using sol-gel method from sodium tungstate, Na_2WO_4, and ion exchange resin. Thin films were prepared using spinner coating technique from the prepared nanomaterials. The effect of number of layers, and additive type; hydrogen peroxide and/or oxalic acid, were investigated. X-ray diffraction (XRD), scanning electron microscopy (SEM), UV-VIS spectrophotometry, Fourier transfer infrared (FTIR), Thermal gravimetric analysis (TGA) and transmission electron microscopy (TEM) were used to characterize different properties of the prepared nanomaterials. Electrochemical measurements were used to evaluate the electrochromic properties. The thickness of the prepared WO_3 thin films was ranged between 0.33 µm to 9.82 µm, depending on the number of applied layers. The crystal structure of pure WO_3 without additive as well as with 4 % oxalic acid exhibited hexagonal structure. Monoclinic structure formed for samples contain 1% hydrogen peroxide and a mixture of 1% hydrogen peroxide and 4% oxalic acid. Hydrogen peroxide and oxalic acid additives led to an open porous structure and increased the diffusion coefficient from $5.3x10^{-14}$ to $3.1x10^{-9}$ cm^2 s^{-1}. High coloration efficiency of 64.2 cm^2 C^{-1} was obtained for the open porous structure of the two-layer film prepared with W^+ ion concentration of 0.1 M, and 1% hydrogen peroxide and 4% oxalic acid.

Keywords: Electrochromic, WO_3, nanomaterials, sol-gel, hydrogen peroxide, oxalic acid

1. INTRODUCTION

Electrochromic devices (ECDs) are optoelectrochemical systems that change their optical properties, mainly their transmittance, when a voltage is applied. This interesting behavior leads to many applications, such as smart windows, sunroofs, shades, visors or rear view mirrors for automotive and mass transportation applications, skylight, displays, light filters and screens for light pipes and other optoelectrical devices [1].

Transition metal oxides have been widely used as inorganic electrochromic materials. Among those transition metal oxides, tungsten trioxide, WO_3, an n-type semiconductor, has been the most extensively studied material due to its electrochromic properties in the visible and infrared region, high coloration efficiency and relatively low price. In recent years, however, there has been an orientation to use chemical rather than physical techniques, which involve high capital investments. Sol-gel or wet chemical synthesis offers many advantages for the preparation of high value added materials in addition to being economically feasible [2]. Sol-gel process is a less expensive route to produce thin films over large areas and offers the advantage of controlling the film microstructure, which strongly affects the kinetics, durability and coloration efficiency [3]. Several sol-gel routes have been developed to produce WO_3 thin films such as acidification of sodium tungstate, peroxopolytungstic acid, and tungsten alkoxide [3]. Hydrated tungsten oxides, $WO_3.nH_2O$, can be obtained via the acidification of a tungstate solution, Na_2WO_4, through a proton exchange resin or directly upon the reaction of sodium tungstate with hydrochloric acid, but it needs to wash out the residual of sodium chloride [4]. The washing step can be avoided by using an ion exchange resin to produce tungstic acid without any side products. A clear solution of tungstic acid, H_2W_4, is first obtained [5], which can be deposited onto the substrate by different techniques, such as, spin coating, spray or dip coating.

The coloration mechanism was studied [6, 7] and both hydrogen peroxide and oxalic acid play great role as stabilizing agents. Luo *et al.* [8] explained that by addition of H_2O_2 into doped tungstic acid caused the formation of peroxo tungstic acid by partly replacing the O^{2-} in $[WO_4]^{2-}$ with O_2^{2-}. This reaction decreased the number of O^{2-} ligands in $[WO_4]^{2-}$, decelerated the condensation among tungstic acid and stabilized the tungstic acid sols. The small ligand molecules $H_2C_2O_4$ could also coordinate with W^{6+} to stabilize the tungstic acid sols, during the formation of tungsten oxide thin films. Particles of tungsten oxide were separated by water and additives molecules, which were evaporated by heat treatment producing porous, as long as the particle size become larger. Also, the pore size enlarged proportionally to the particle size. Various applications of WO_3 thin films require different types of crystalline structure. Electrochromic devices employ both amorphous as well as crystalline WO_3 films owing to their high catalytic behavior both in oxidation and reduction processes [9]. Shiyanovskaya [7] supposed that the injected electron is trapped at a W^{6+} site adjacent to a proton thus forming W^{5+} color center. Light absorption occurs due to charge transfer between two neighboring tungsten sites, W^{5+} and W^{6+}. Injected protons compensate for the negative charge of injected electrons [7].

It has been realized that the morphology and structure of WO_3 directly relate to its ability to perform the desired function in a particular application [10]. So, the electrochromic properties like coloration efficiency, cyclic durability, and kinetics of coloration–bleaching process of tungsten trioxide strongly depends on its structural, morphological, and compositional characteristics [9].

This investigation aims to prepare and study WO_3 thin films via sol-gel route using spinner coating technique. Number of coating layers, additive type; hydrogen peroxide and/or oxalic acid were the main parameters used to explore the coloration efficiency of the prepared films. The tungstic acid is obtained via the acidification of a tungstate solution, Na_2WO_4, through a proton exchange resin, then tungsten oxide thin films were spin coated from the tungstic acid and annealed at 300 $^{\circ}$C for 30 min. The effect of hydrogen peroxide and oxalic acid on the performance of WO_3 thin films is studied and summarized in Table 1.

Table 1. WO_3 thin films preparation conditions and performance

Sample	Sample 1	Sample 2	Sample 3	Sample 4
	Without additive	1% hydrogen peroxide	4% oxalic acid	1% hydrogen peroxide and 4% oxalic acid
	W^+ ion concentration 0.1 M, spinner coated at 200 rpm for 60 seconds, and heat treated at 300 °C for 30 minutes			
Transmittance T% (at 550 nm)	82.4	90.4	79.6	87.7
Diffusion coefficient (C/cm^2)	5.3×10^{-14}	8.3×10^{-14}	4.2×10^{-10}	3×10^{-09}
Coloration Efficiency (cm^2/C)	8.5	19.5	45.2	63.6
Purity	pure	1% hydrogen	4% oxalic	both
2 theta	23.0	23.0	35.5	37.7
Size (nm)	46	50	45	12
Plane	001	110	201	211

2. EXPERIMENTAL SECTION

2.1. Preparation of WO_3 thin films

Tungsten oxide was formed via the acidification of 0.1M sodium tungstate (98%, Sisco research laboratory, India) through a proton exchange resin (Rohm& Haas, France) to produce a solution of tungstic acid. 0.1M H_2O_2 and 0.1M oxalic acid was added as 1% and 4% volume ratio, respectively. The obtained solution was deposited by spin coating (Polos 300 AWS- CPK Industries, USA) at 200 rpm for 60 seconds and annealed at 300 °C for 30 min in open air furnace (Carbolite, Aston Iane, Hope Sheffield, 53 2RR, England) to produce a single layer or multi-layers of tungsten oxide thin film.

2.2. Characterization of WO_3 thin films

X-ray diffraction patterns of the obtained films were obtained by X-ray diffractometer (Schimadzu -7000, USA), operating with Cu-kα radiation (λ = 0.154060 nm) generated at 30 kV and 30 mA. The scan rate was (2^o / min.) for 2θ values between 20 and 80 degrees. The surface morphology and analysis of the film was investigated with high resolution scanning electron microscopy (JEOL JSM 6360LA, Japan). Thin films of gold were sputtered onto the samples to get charge free surfaces. Also, measurements of various grain sizes and film thickness were estimated from the SEM micrographs. The transmission (T) and absorption (Abs) of the prepared thin films were measured using Double beam UV – VIS Spectrophotometer (Labomed, USA). The measurements were carried out in the range 190-1100 nm at room temperature. Vibrational spectroscopic studies for as-deposited and annealed WO_3 thin films were obtained by FTIR spectrophotometer (Schimadzu -

8400 s - Japan) at room temperature in the frequency range 4000–500 cm^{-1}. Thermal properties of WO_3 upon annealing were studied by thermogravimetric analysis (TGA 50, Shimadzu, Japan). Transmission electron microscopy (TEM) (JEOL JEM 1230, Japan) operating at 12-600 kV was used to determine the size of WO_3 nanoparticles, WO_3 thin film was stripped off from glass substrate and suspended in ethanol, then spread onto copper grid for TEM measurement.

2.3. Electrochromic properties of WO_3 thin films measurements

The electrochemical set-up consists of a Potentiostat (Voltalab PGP201 - Radiometer Analytical - France) controlled by a computer and conventional three-electrode cell in which the saturated calomel electrode (SCE) and a platinum wire were used as reference and counter electrodes, respectively. Tungsten oxide on ITO coated glass was used as the working electrode in an electrolyte solution of lithium perchlorate (98%,Fluka, Switzerland) / propylene carbonate (PC) (99%, Aldrich, Germany) of 1M ($LiClO_4$: PC). The CV's were recorded in the range 0-1 V versus (SCE) with a scan rate of (10 mV/s). All the measurements were carried out at room temperature and the cyclic voltammograms were recorded after 10 activation cycles. Electrochromic measurements were recorded using a system consists of Potentiostat and spectrophotometer by connecting samples to Potentiostat when placed inside the spectrophotometer measurement compartment, and by applying a current of (I = 1mA) in a solution of 1M $LiClO_4$/PC for 60 sec and recording the change in transmittance at λ=550 nm, at room temperature.

3. RESULTS AND DISCUSSIONS

3.1. X-Ray Diffraction

Fig. 1 shows XRD patterns of WO_3 thin films prepared using different preparation conditions. Pure WO_3 thin films with no additives (Fig. 1a), reveals the hexagonal WO_3 structure (JCPDS card no. 33-1387). High orientation of the (001) plane at $2\theta = 23.03^o$ is detected. Adding 4% of oxalic acid (Fig.1b) improves the crystallinity of WO_3 hexagonal structure and most of the planes are well identified with high orientation of (100), (001) and (201) planes detected at $2\theta = 13.26º$, 23.03º and 35.5º, respectively. Deepa *et al.* [11] explain that oxalic acid upon subliming out of the film catalyzes the formation of crystalline phase at lower temperature. When adding 1% H_2O_2 during WO_3 preparation, semi-amorphous structure with weak peaks of the monoclinic WO_3 structure (JCPDS card no. 54-0508) is detected as shown in Fig. 1c. Adding both 1% H_2O_2 and 4% oxalic acid, improve the crystallinity of the semi-amorphous structure with high orientation of (100) and (211) planes detected at $2\theta = 25.38º$ and 37.38º of the monoclinic structure.

The average crystallite size was calculated from the full width at half maximum (FWHM) of the diffraction peak using Debye- Scherrer's equation [11] and summarized in Table 1. The obtained pure WO_3 thin films have crystalline size of 46.2 nm increased to 49.8 nm be adding 1% hydrogen peroxide and decreased to 44.5 nm by adding 4% oxalic acid and decreased sharply to 12.3 nm by

adding both of 1% hydrogen peroxide and4% oxalic acid, with good agreement with TEM image (Fig.3 b).

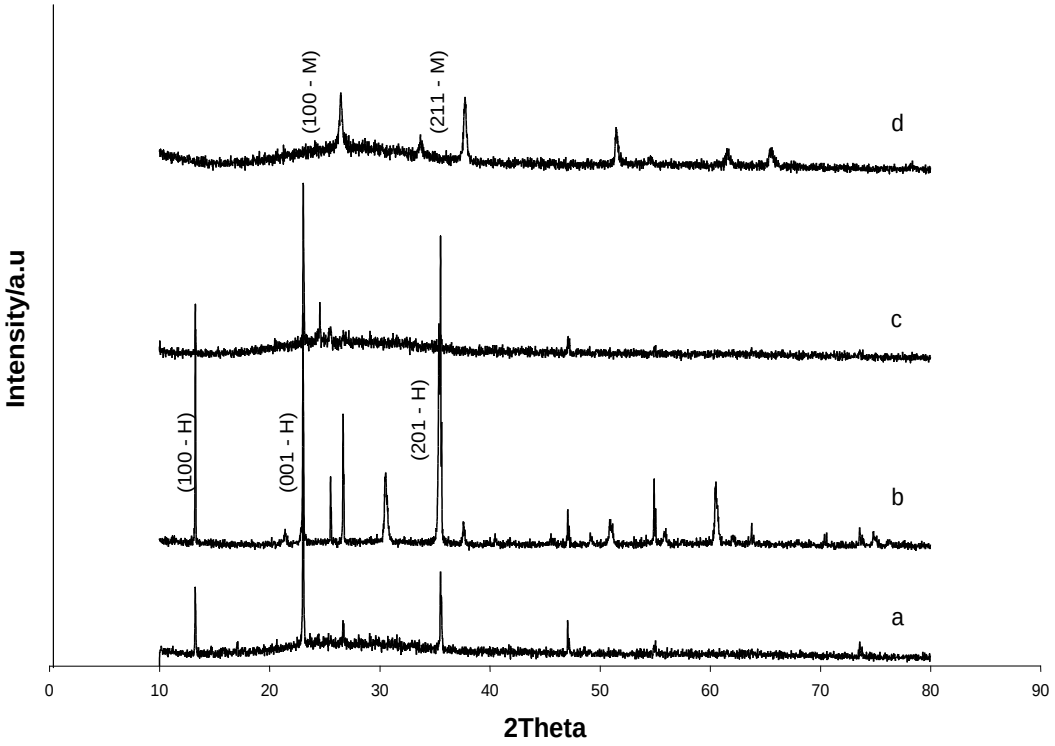

Figure 1. XRD patterns of WO_3 thin films (a) pure (b) 4% oxalic acid (c) 1% hydrogen peroxide (d) 1% hydrogen peroxide and 4% oxalic acid

3.2. Morphology Measurements

Fig. 2 shows the SEM micrographs of WO_3 thin films prepared under the same conditions as in Fig.1. Smooth and uniform films are observed for the WO_3 thin films prepared with pure (Fig. 2a) and with adding 1% H_2O_2 (Fig. 2b). With the addition of 4% oxalic acid (Fig. 2c) and both 1% H_2O_2 and 4% oxalic acid (Fig. 2d), the prepared thin films exhibited porous structure. These additives have the advantage of getting crackles thin films of WO_3, as explained by Nidhi *et al.* [12].

Fig. 3 Shows low magnification TEM of the WO_3 nanoparticles. With no additives (Fig. 3a), the particles are agglomerated in spherical shape with a diameter of 50 - 200 nm. Adding 1% H_2O_2 (Fig. 3b), rod shape with a diameter of about 20 nm and length of 100 nm is observed. Finally, adding 1% H_2O_2 and 4% oxalic acid (Fig. 3c), nanorods were detected with increasing their aspect ratio to 6-7. Fig. 4 shows high magnification TEM images of WO_3 nanoparticles. With 4% oxalic acid, (Fig. 4a) small nanoparticles of 7-8 nm and 20 nm were found. Adding 1% H_2O_2 and 4% oxalic acid (Fig. 4b), nanoparticles of 7-12 nm in good agreement with results obtained from XRD (Table 1).

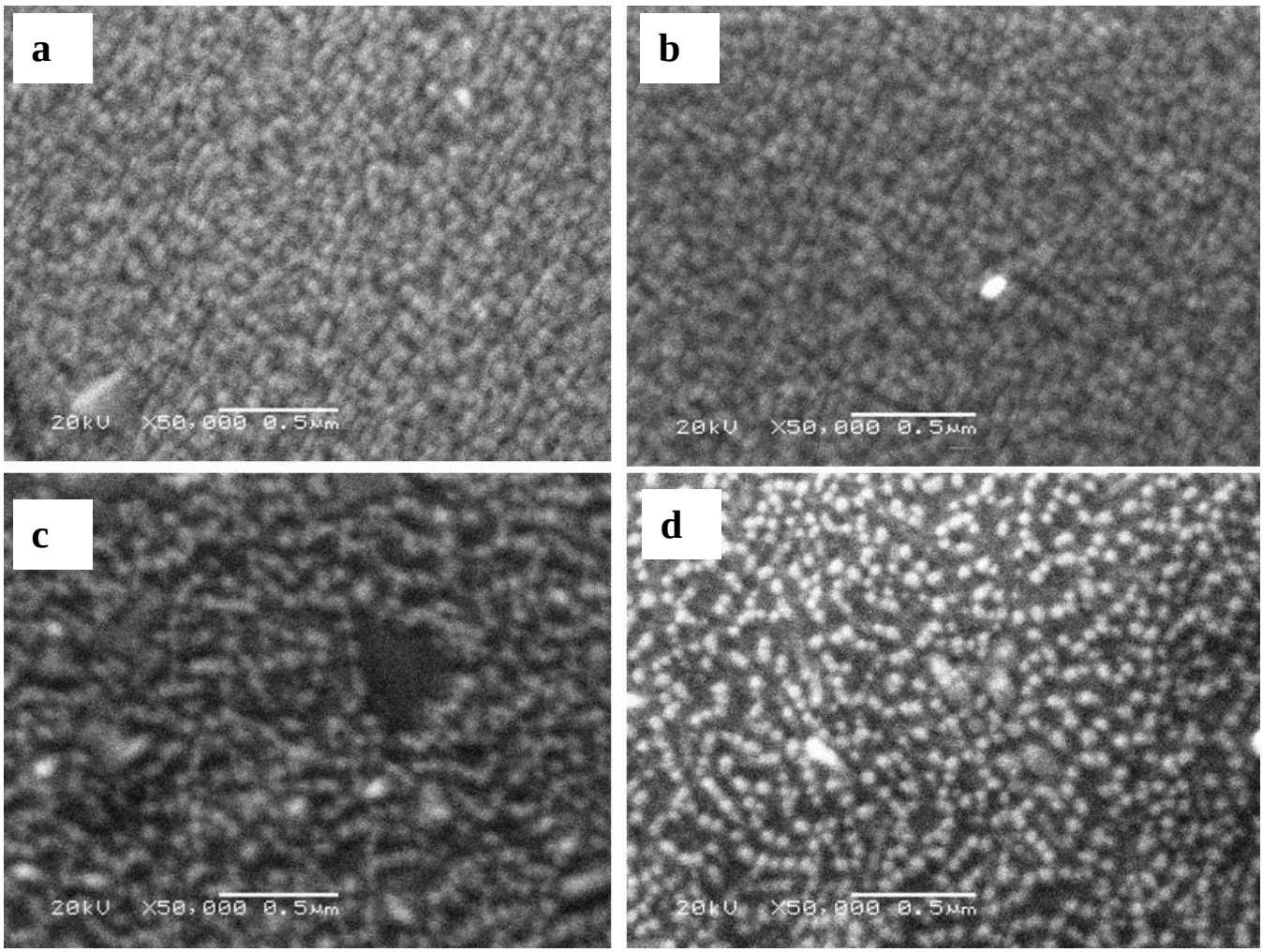

Figure 2. SEM micrograph of WO_3 thin films (a) pure (b) 1% hydrogen peroxide (c) 4% oxalic acid (d) 1% hydrogen peroxide and 4% oxalic acid

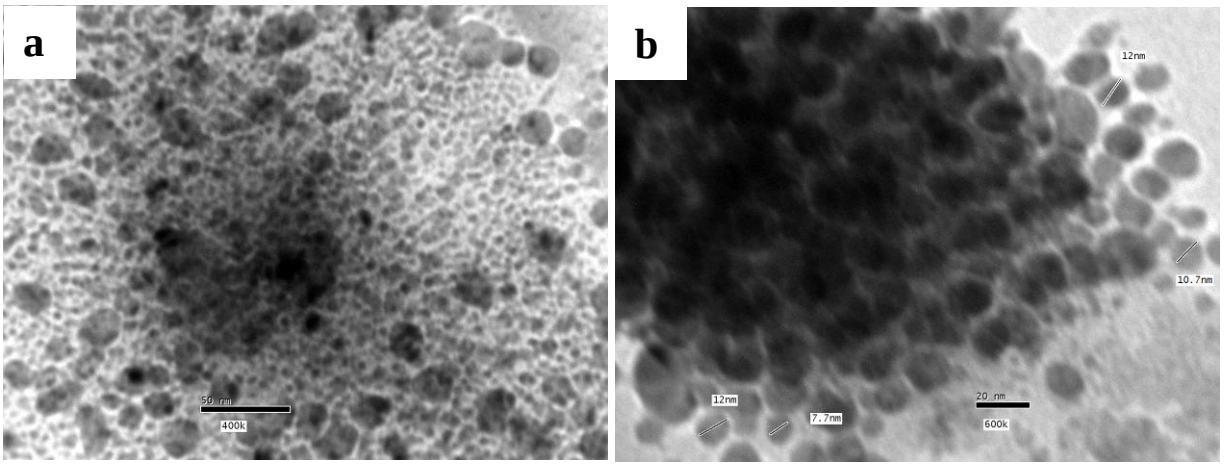

Figure 3. High magnification TEM images of WO_3 nanoparticles prepared at different additives concentrations; (a) 4 % oxalic acid (b) 1 % H_2O_2 and 4 % oxalic acid

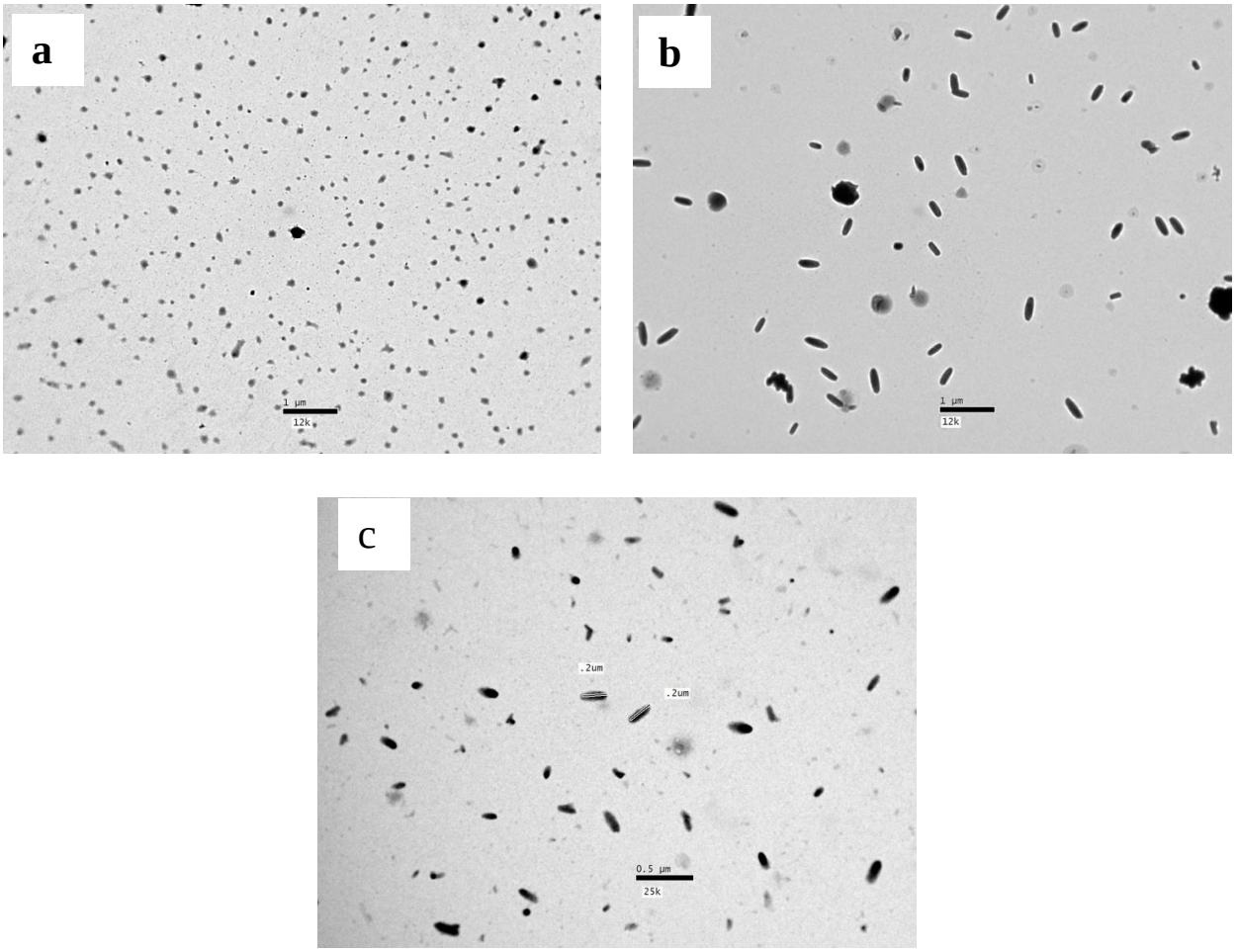

Figure 4. Low magnification TEM images of WO_3 nanoparticles prepared at different additives concentrations; a) No additives, b) 1 % hydrogen peroxide and c) 4 % oxalic acid

3.3. Thermal measurements

Fig. 5 shows the results obtained from WO_3 samples. No weight loss of all samples annealed at 300^{o}C (Fig. 5e), while samples prepared without annealing show slight weight loss (about 3-7 %) at temperature range (90 -180^{o}C) due to an evaporation of physically adsorbed water and solvent molecules [11], while the major weight loss (about 2-10 %) at (180-260^{o}C) was attributed to the loss of chemically bonded water of crystallization [4]. The amount of lost water increased under influence of additives, the maximum water loss was in the case of using 1% H_2O_2 and 4% oxalic acid as demonstrated by FTIR spectra (Fig. 6). This may be due to adsorption of water by porous structure as remarked in SEM micrographs, Fig. 2.

3.4. FTIR Measurements

Fig. 6 shows FTIR spectra of WO_3 thin films with different additives. Peak at 3442 cm^{-1} is referred to water, which increased by adding additives due to porous structure as illustrate by SEM

micrographs (Fig. 2), and TGA measurements (Fig. 5). WO_3 prepared by adding oxalic acid was characterized by the strong band at 1545 cm^{-1} corresponding to COO group [13] as shown in Fig. 6c and 6d. There is almost no deference between Fig 6c and 6d, which indicate that hydrogen peroxide has no effect on sample prepared by adding oxalic acid that has more chemical stability due to delocalized negative charge on the two oxygen atoms. Peak at 628-630 cm^{-1} is referred to O-W-O; Vijayalakshmi *et al.* [14] recorded the same pack at 674 cm^{-1} for electrodeposited WO_3 thin films. Peak at 977 cm^{-1} is referred to W=O, in good agreement with results obtained by Deepa *et al.* [11].

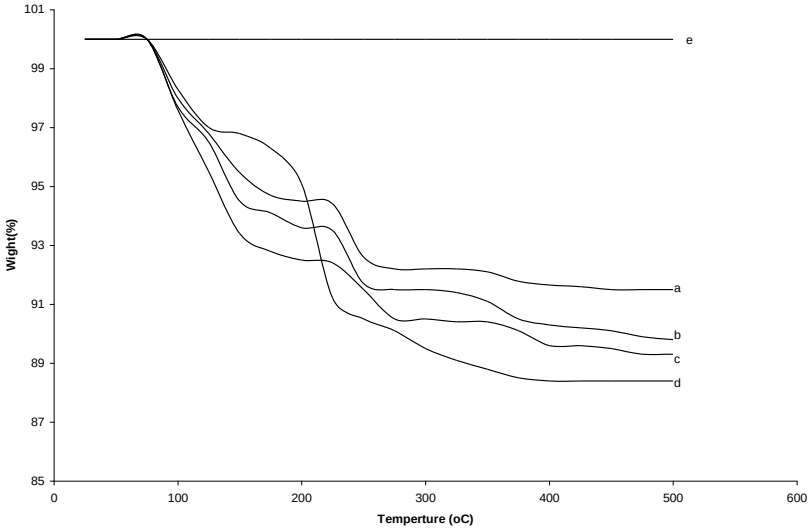

Figure 5. TGA plots of WO_3 thin film without annealing (a) pure, (b) 1% hydrogen peroxide, (c) 4% oxalic acid, (d) 1% hydrogen peroxide and 4% oxalic acid, and (e) after annealing at 300^{o}C for 30 minutes

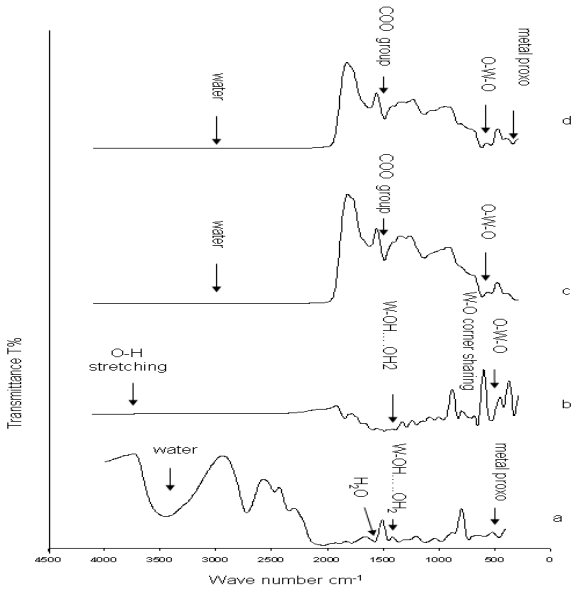

Figure 6. FTIR spectra of WO_3 thin films (a) pure, (b) 1% hydrogen peroxide, (c) 4% oxalic acid, and (d) 1% hydrogen peroxide and 4% oxalic acid

3.5. Optical Measurements

Fig.7 reviews the effect of additives on WO_3 thin films transmittance spectra. The pure WO_3 thin film (Fig. 7a) shows some interference fringes due to smooth surfaces due to uniform distribution of WO_3 particles on the substrate (Fig. 2a), which disappears in the other thin films due to some roughness caused by additives (Fig. 2b, c, d).

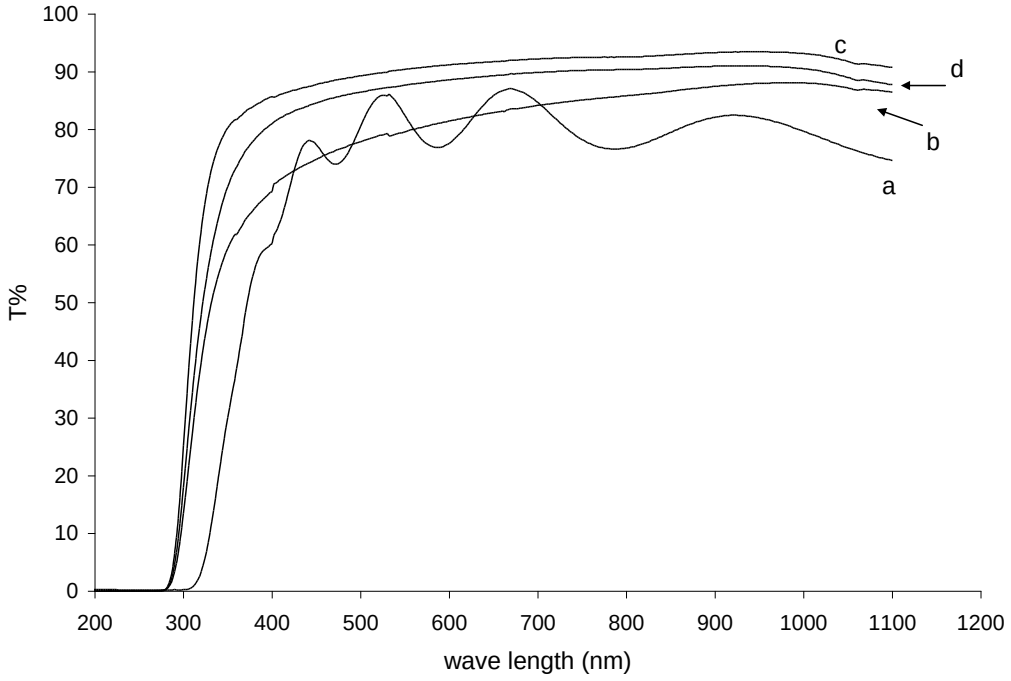

Figure 7. Transmittance spectra of WO_3 thin films (a) pure, (b) 4% oxalic acid, (c) 1% hydrogen peroxide, and (d) 1% hydrogen peroxide and 4% oxalic acid

3.6. Electrochemical Measurements

Cyclic voltammetry was used to obtain the electrochemical properties of WO_3 thin films under oxidation state. The main parameter that will be determined from cyclic voltammetry is the current peak i_p, which depends strongly on the diffusion coefficient. Anodic peak refers here to the current peak caused by insertion of Li^+ ions into the WO_3 thin films, while the cathodic peak refers to exertion of Li^+ ions.

Fig. 8 shows the cyclic voltamograms of WO_3 thin films. It is observed that the anodic peak increased by adding hydrogen peroxide and oxalic acid due to open porous structure as explained by Z. Ya *et al.* [15]. Wei Cheng [16] explained that the charge transfer depends on the proton – injecting contact (electrolyte - WO_3 interface), surface area, pore size and the porosity affected by additive as shown in Fig. 2.

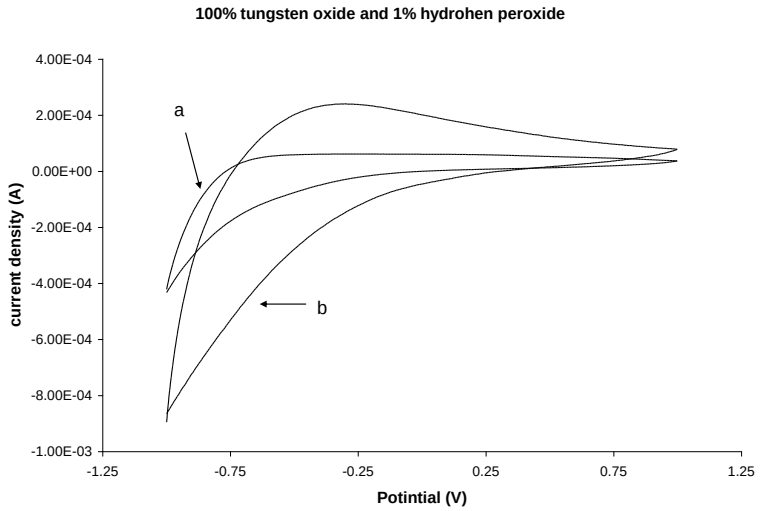

Figure 8a. Cyclic voltammogram of WO_3 thin films (a) pure, (b) 1% hydrogen peroxide

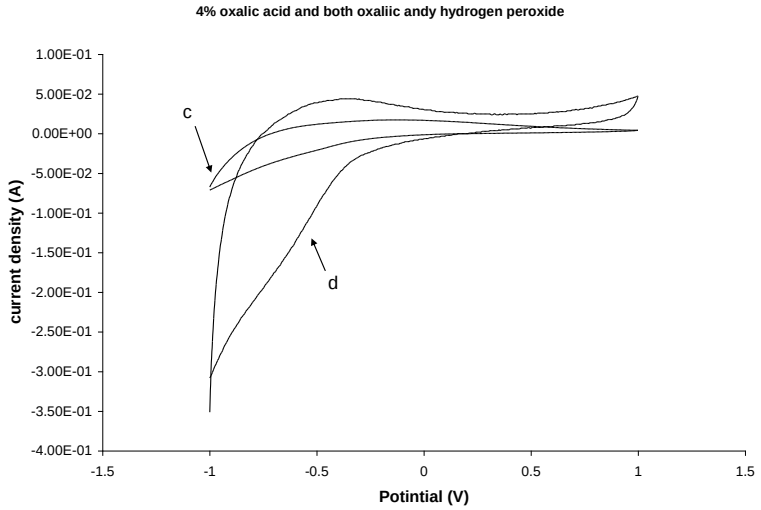

Figure 8b. Cyclic voltammogram of WO_3 thin films (c) 4% oxalic acid, and (d) 1% hydrogen peroxide and 4% oxalic acid

The diffusion coefficient, D, of lithium ions (Li^+) was calculated using Randles-Sevcik equation [17]:

$$i_p = 2.69 x 10^5 n^{3/2} A D^{1/2} C v^{1/2} \quad (1)$$

Where i_p is the anodic peak current (Amp.) at oxidation state, n is the number of electrons transferred (n = 1 in this case), A is the electrode area (cm^2), D is the diffusion coefficient (cm^2/s), C is the concentration of the electrolyte (mol/cm^3), and ν is the voltage scan rate (V/s). Table 1 gives the diffusion coefficient values for WO_3 thin films prepared with different additives. The highest diffusion coefficient is $3.05x10^{-9}$ cm^2/C that recorded for the sample with 1% hydrogen peroxide and 4% oxalic

acid. The water content and the porosity play a great role in the diffusion coefficient by increasing the diffusion coefficient value with H^+ ions.

The transmittance that the human eye perceives is called luminous and the maximum sensitivity corresponds to the photon wavelength of 550 nm. The coloration efficiency, η, was calculated at constant λ=550 nm by applying constant current (I = 1 mA) in a solution of 1M $LiClO_4$/PC for 60 seconds.

The charge, Q, which was inserted into the sample, (area, A = 3 cm^2) is:

$$Q = I\,x\,t = 0.001x60 = 0.06C, Q/A = 0.06/3 = 0.02C/cm^2 \quad (2)$$

η can be calculated as follows:

$$\eta = \frac{\Delta OD}{\Delta Q} = \frac{\log(T_b / T_c)}{(Q/A)} (\text{cm}^2/\text{C}) \quad (3)$$

Where ΔOD is the optical density difference, T_b and T_c are transmittance at colorless and colored status, respectively as shown in Fig. 9, Q is the inserted charge, and A is the electrode area.

Table 1 summarizes the results of coloration efficiency, presenting the highest calculated coloration efficiency in this work to be 63.6 cm^2/C for sample with 1% hydrogen peroxide and 4% oxalic acid. These results is close to results obtained by our previous work [18] and higher than other results (34 - 47.6 cm^2/C) obtained by Deepa *et al.* [11], while Zayim got coloration efficiency of (63 cm^2/C) by sol gel starting from WCl_6 at 650 nm with 1% TiO_2 [19].

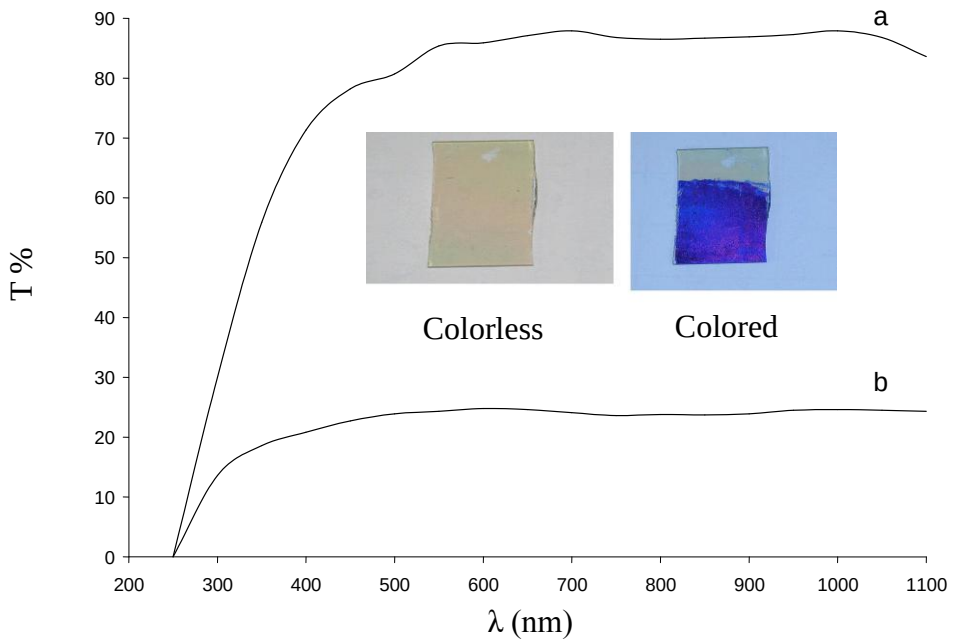

Figure 9. Transmittance spectra of WO_3 thin films with 1% hydrogen peroxide and 4% oxalic acid at (a) colorless state and (b) colored state

Fig. 10 shows the coloration efficiency of WO_3 thin films with 4% oxalic acid and 1% H_2O_2 and 4% oxalic acid over number of cycles. It is noted that the coloration efficiency decrease by increasing the number of cycles, which may be due to formation of non-reversible component of Li_2O.

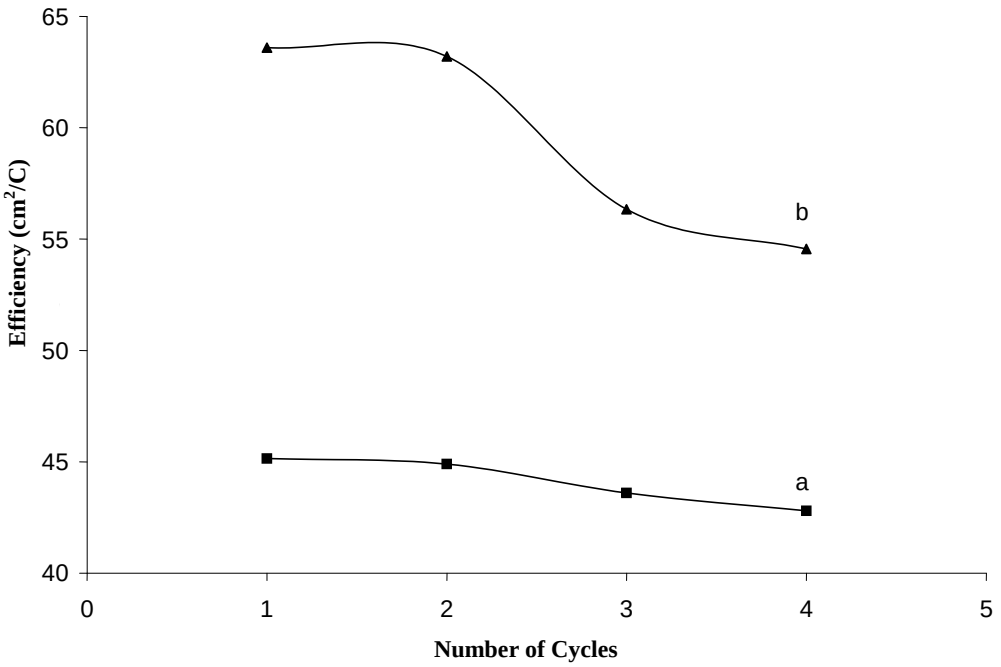

Figure 10. Coloration efficiency of multi cycled WO_3 thin films with (a) 4% oxalic acid and (b) 1% H_2O_2 and 4% oxalic acid

3.7. Thickness measurements

Table 2 and Fig. 11 a-e summarize and show the thickness of multi-layers of WO_3 with 1% hydrogen peroxide and 4% oxalic acid thin films and the coloration efficiencies of these films. The highest coloration efficiency (64.2 cm^2/C) was recorded for two layers of WO_3 thin film, which may be due to the microstructure of this layers, and the cave between layers increase the migration of Li^+ ions throw the film and increase the coloration efficiency as shown in Fig. 11b. Other samples don't such porous microstructure and therefore have low coloration efficiency.

Table 2. Thickness of multi-layers of WO_3 with 1% hydrogen peroxide and 4% oxalic acid thin films and their coloration efficiency

No. of layers	1	2	4	6	8
Thickness (μm)	0.17–0.33	1.6–1.8	4.38–4.95	6.36–6.4	8.39-9.82
Efficiency (cm^2/C)	63.6	64.2	50.5	43.9	38.3

4. CONCLUSIONS

In this research, electrochromic WO_3 thin films were deposited by spin coating from a solution of tungstic acid obtained using ion exchange method.

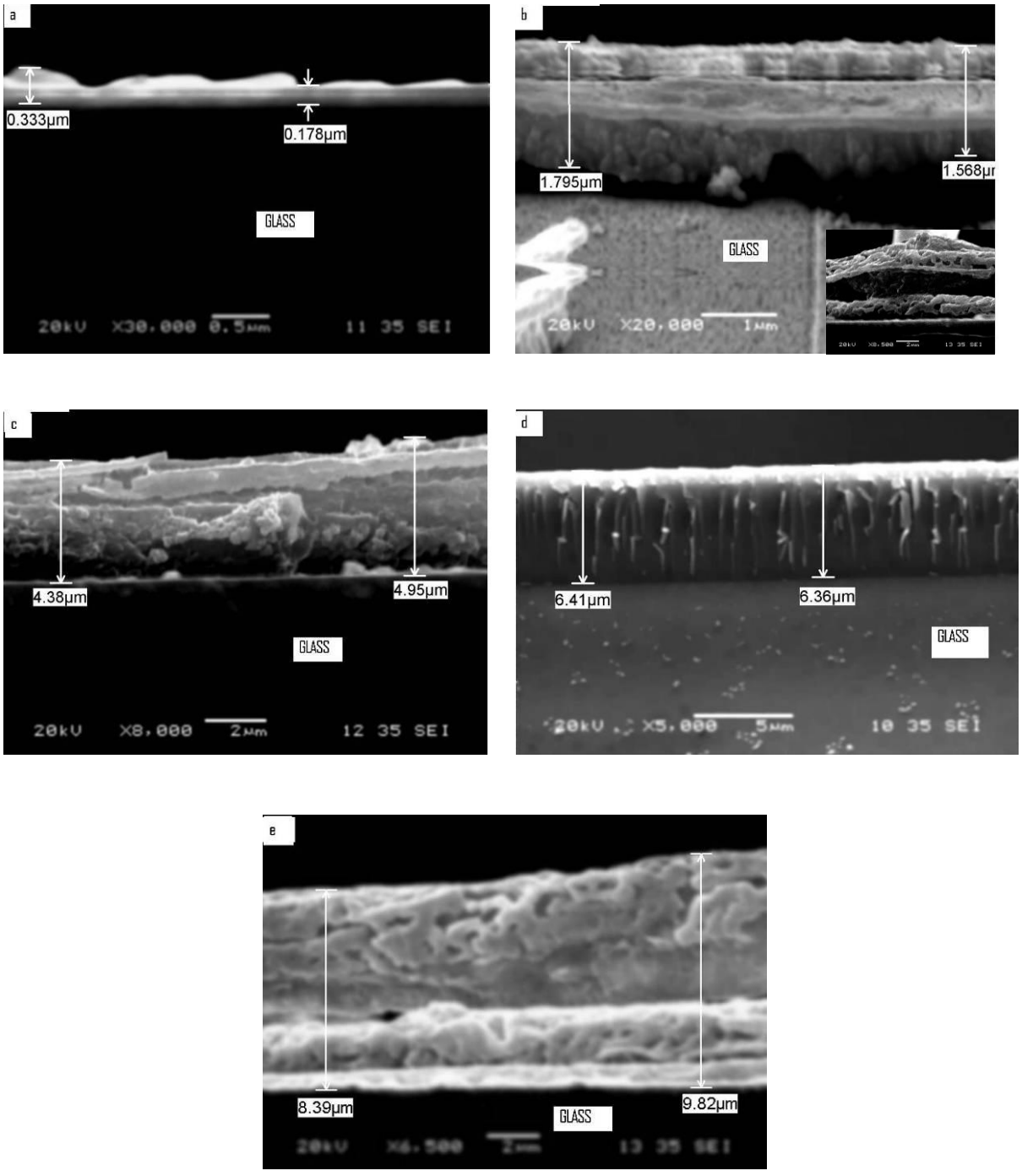

Figure 11. Cross-section SEM micrograph of (a) one layer of WO_3 thin film (b) two layers (c) four layers (d) six layers (e) eight layers

The obtained thin films have low pores structure (monoclinic) which turned to open pores structure (hexagonal) by adding 1% of hydrogen peroxide and 4% of oxalic acid. These additives also increased the transmittance, diffusion coefficient and coloration efficiency. Coloration efficiency was affected also by number of layers, and the highest coloration efficiency (64.2 cm^2/C) was recorded for two layers of WO_3 thin film.WO_3 shape turned from spherical nanoparticle with diameter of 50-200 nm to rod with diameter of 20-50 nm by adding 1% H_2O_2, and finally to rod with diameter of 100-200 nm and length of 200-500 nm by adding 4% oxalic acid.

ACKNOWLEDGMENTS

The authors gratefully acknowledge the staff of Mubarak city for scientific research and technology applications (MuCSAT) for funding this work among the internal project of electrochemistry and nanotechnology. Also, the acknowledgement goes to the Egyptian Science and Technology Development Fund (STDF) for funding this work among the STDF project No. 277.

References

1. Cesar O. Avellaneda, Diogo F. Vieira, Amal Al-Kahlout, Sabine Heusing, Edson R. Leite, Agnieszka Pawlicka, Michel A. Aegerter, *Solar Energy Materials & Solar Cells* 92(2008) 228-233.
2. S.A. Agnihotry, N. Sharma and M. Deepa, *Sol-Gel Science and Technology* 24(2002) 265–270.
3. C´Esar O. Avellaneda, *Sol-Gel Science and Technology* 19 (2000) 447–451.
4. Sitthisuntorn Supothina, Panpailin Seeharaj, Sorachon Yoriya, Mana Sriyudthsak, *Ceramics International* 33(2007) 931-936.
5. J. Liuage. G. Gu Man, *Solid State Ionics* 84 (1996) 205-211.
6. C. G. Granqvist, E. Avendaño, A. Azens, *Thin Solid Films* 442 (2003) 201–211.
7. I.V. Shiyanovskaya, *Non-Crystalline Solids* 187 (1995) 420-424.
8. Wei Luo, Xiang Kai Fu, Li Hua Ma, *Chinese Chemical Letters* 18 (2007) 883–886.
9. K.J. Patel, C.J. Panchal, V.A. Kheraj, M.S. Desai , *Materials Chemistry And Physics* 114 (2009) 475–478.
10. Wei Xiaolan, Shen Peikang, *Science In China Ser. B Chemistry* 48 (2005) 511—514.
11. M. Deepa, T.K. Saxena, D.P. Singh, K.N. Sood, S.A. Agnihotry, *Electrochimica Acta* 51 (2006) 1974–1989.
12. Nidhi Sharma, M. Deepa, Pradeep Varshney, S. A. Agnihotry, *Sol- Gel Science and Technology* 18 (2000) 167-173.
13. A.Patra, K. Auddy, D. Ganguli, J. Livage, P. K. Biswas, *Materials Letters* 58 (2004) 1059–1063.
14. R. Vijayalakshmi, M. Jayachandran, C. Sanjeeviraja, *Current Applied Physics* 3 (2003) 171–175.
15. Zhenrui Yu, Xiaodong Jia, Jinhui Du, Jiayou Zhang, *Solar Energy Materials & Solar Cells* 64 (2000) 55-63.
16. Wei Cheng, Emmanuel Baudrin, Bruce Dunna and Jeffrey I. Zink, *J. Mater. Chem.*, 11 (2001) 92-97.
17. A.K. Srivastava, M. Deepa, S. Singh, R. Kishore, S.A. Agnihotry, *Solid State Ionics* 176 (2005) 1161–1168.
18. H.M.A. Soliman, A.B. Kashyout, Mohamed S. El Nouby, A.M. Abosehly, *J. Mater. Sci: Mater Electron*, DOI 10.1007/s 10854-010-0068-0.
19. Esra Ozkan Zayim, *Solar Energy Materials & Solar Cells* 87 (2005) 695–703.